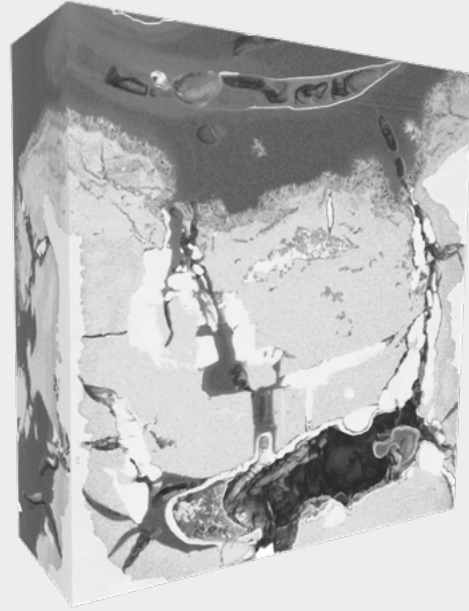




500 μm



10 μm

## Multi-scale Correlative Study of Corrosion Evolution in a Magnesium Alloy

# Multi-scale Correlative Study of Corrosion Evolution in a Magnesium Alloy

---

Author: William Harris  
Carl Zeiss X-ray Microscopy, Inc.

---

Date: January 2019

---

This work was performed in collaboration with researchers from the University of Manchester, School of Materials, including Heike Krebs, Professor George Thompson, Dr. Ali Chirazi and Professor Philip Withers.

---

**Here we describe the results of a multi-scale correlative tomography study on corrosion of a Magnesium alloy that uses Atlas 5 to efficiently link and navigate between *in situ* sub-micron X-ray microscopy, nanoscale X-ray microscopy and FIB-SEM tomography. The results point to a detailed description of the complex crack and corrosion by-product geometries which can lead to a more complete understanding of the underlying mechanisms for corrosion.**

## Introduction

Magnesium alloys serve as lightweight, high strength alternatives to Al and Ti based alloys for certain applications, notably in the automotive and aerospace industries. However, the high production cost of Mg alloys coupled with the influence of impurities and alloying elements on their corrosive properties, have limited their widespread usage. These issues motivate the need to understand and control the impurities, including their distribution and morphology, as well as the overall alloy microstructure and degradation processes. X-ray microscopy (XRM), a nondestructive 3D imaging technique, is first used in this study to understand the time-dependent evolution and overall extent of corrosion damage in the surface and sub-surface regions. By probing the internal structure without the need for complex sample preparation and physical sectioning techniques, XRM presents unique opportunities to understand the dynamics and mechanisms of material degradation. Subsequently, selectively targeting regions of interest for examination with nanoscale XRM and FIB-SEM tomography reveals the extent and nature of corrosion damage at nanometer length scales. Here we demonstrate an efficient 3D correlative tomography workflow, powered by ZEISS Atlas 5 to spatially register and guide subsequent stages of microstructural investigation, moving from sub-micron XRM to nanoscale XRM, finally to FIB-SEM. This coordinated workflow approach is essential in making complex multi-scale experiments approachable in an efficient time frame, maximizing the output of each imaging modality.

## Corrosion of Mg Alloys

Magnesium alloys are commonly used in automotive and aerospace applications due to their light weight and high strength. However, the alloys can corrode in humid or wet environments, particularly when salt is present. [1] The associated damage can occur by a number of mechanisms, including pitting and intergranular corrosion, and is frequently attributed to the presence of impurities and intermetallic compounds within the alloys. These phases can serve as cathodic reaction sites, forming microgalvanic cells with the surrounding magnesium. Therefore, understanding the coupling between microstructural features and corrosion damage is important to developing new processes and alloy compositions to mitigate these detrimental effects. [2,3]

Furthermore, while corrosion is the result of an electrochemical process occurring at a surface, prolonged exposure to a corrosive environment can quickly lead to progressive damage extending into the depth of the material. As a result, the degradation is no longer limited to a 2D effect, but can become a highly irregular 3D process depending on the dominant corrosion mechanisms. Consequently, comprehensive characterization requires multiple imaging approaches, spanning several length scales in both 2D and 3D. In this study, 3D imaging is implemented by X-ray microscopy and FIB serial section tomography across a range of length scales from mm to nm.

#### 4D and Multiscale Imaging Procedure

An overview of the experimental procedure is shown in Fig. 1.

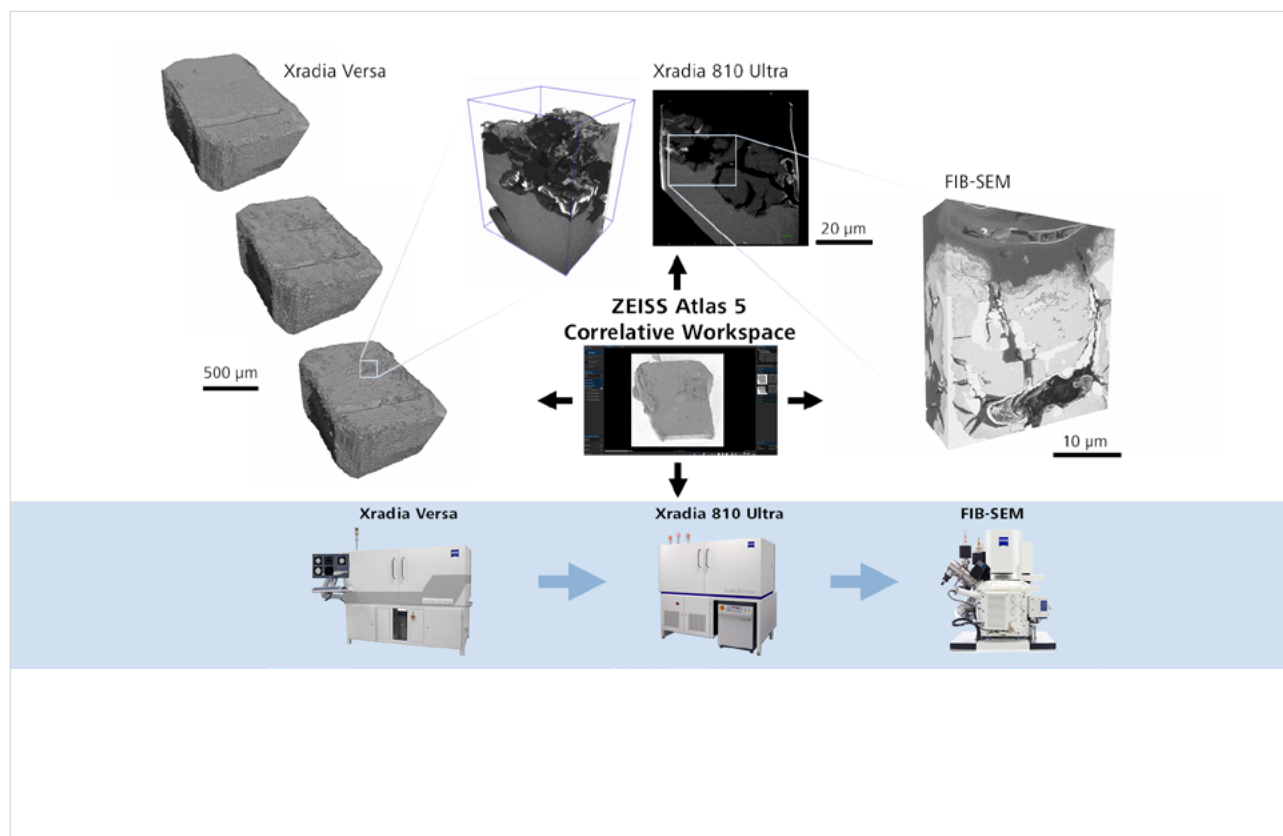


**Figure 1** Experimental Overview. This multiscale correlation study was designed to better understand corrosion damage in a Mg AZ31B alloy sample. The Atlas 5 correlative workspace was used to link and navigate between imaging performed on Xradia Versa, Xradia 810 Ultra, and FIB-SEM microscopes.

A sample of AZ31 alloy (approx. 3 % Al, 1 % Zn, 0.2 % Mn, 0.1 % Si, trace Ca, Cu, Fe, Ni, and balance Mg) was cut to a square cross section of approximately 1 mm x 1 mm, with thickness of 2 mm. The top surface was not modified, while the remaining surfaces were coated in a protective resin to allow corrosion from only the single direction. The sample was immersed in a 0.1 M NaCl solution, placed in a ZEISS Xradia Versa X-ray microscope, and imaged *in situ* with an isotropic voxel size of 1 micron at a rate of two hours per scan. The plastic chamber and salt solution provided minimal attenuation of X-rays, and therefore did not have a detrimental impact on the XRM imaging. Because the corrosion process was proceeding continuously, each tomographic data set was not a perfect static structure, but rather was representative of the average extent of the corrosion damage in the given two hour window. The scans were set to repeat continuously with the same parameters and

sample position, and the results were analyzed following each scan to determine when the corrosion process transitioned from a surface and near-surface effect to more substantial progression into the depth of the bulk material. When onset of this transition was observed, the sample was removed from the chamber and rinsed with distilled water to stop the corrosion process.

In order to observe the damaged regions in more detail, the sample was first mounted in a ZEISS FIB-SEM. The final 3D Versa data set of the 4D *in situ* time series was imported and aligned to the SEM surface view using the ZEISS Atlas 5 correlative microscopy software. The Atlas 5 platform simultaneously serves as a correlative analysis environment by collating data acquired across numerous instruments, but also uniquely controls the FIB-SEM imaging and acquisition tasks based directly on the data loaded in the correlative

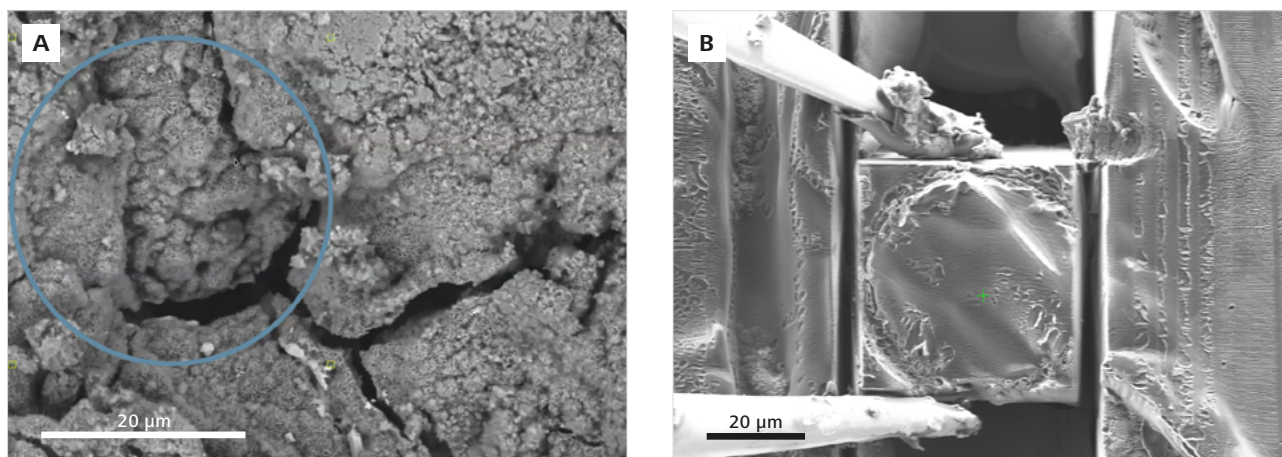


**Figure 2** a) The blue circle denotes the region of interest selected for higher resolution imaging. b) After coating the surface of the sample with a protective epoxy layer, Atlas 5 was used to navigate to the same region of interest and drive the FIB-SEM to extract a pillar sample with a cross section of approximately  $50\ \mu\text{m} \times 50\ \mu\text{m}$ .

workspace. [4] In this study, a combination of the 3D XRM data and the high resolution 2D SEM surface view were used to locate and define a highly corroded region of interest, as shown by the green circle in Fig. 2a. The sample was then removed from the electron microscope and coated in a thin layer of epoxy to preserve the fine porous structures during subsequent FIB milling. After re-mounting in the FIB-SEM, Atlas 5 was used to navigate to the same region of interest defined previously, despite the fact that the visible surface topology changed substantially due to the epoxy coating. This was achieved using Atlas 5's image registration features to align the epoxy-coated sample with the previously acquired image of the uncoated surface. At this target location, a sub-sample of approximately  $50 \times 50 \times 80\ \mu\text{m}$  was extracted using the FIB-SEM lift-out method, as shown in Fig. 2b. A microgripper was used to hold the sample during the final cut, and then transfer the sample to the tip of a needle where it was attached with SEM glue which hardens under electron beam irradiation. This sub-sample was then imaged in the ZEISS Xradia 810 Ultra XRM, in order to extend the 3D imaging down to a resolution of 150 nm with a FOV of  $65\ \mu\text{m}$ .

Following nanoscale tomography in ZEISS Xradia Ultra, the sample was again mounted in the FIB-SEM to collect a 3D FIB tomography at a targeted location with an 8 nm voxel size. The FIB tomography was performed at a specific

site of significant grain boundary corrosion to examine the fine structural features at this length scale, below the resolution of the X-ray imaging techniques.

#### Analysis of Corrosion Damage

The data obtained from the *in situ* study performed on ZEISS Xradia Versa revealed initial widespread pitting across the surface of the sample in the first several hours, as shown in Fig. 3a and 3b. (The black arrow denotes a fiducial mark used for reference on the sample surface.) The pits became increasingly widespread covering much of the surface. This initial damage, dominated by surface and very near surface processes, has been denoted as 'Stage 1' corrosion. By the 14 hour mark, there became evidence of an emergence of so-called 'Stage 2' corrosion, in which further surface damage appeared to slow in favor of increased expansion of the corrosion front into the depth of the material. This is evident in the final ZEISS Xradia Versa data set of Fig. 3c and 3d, showing the increased local sub-surface degradation just below the surface features. Fig. 3d also reveals a cutaway view of the interior of the sample, revealing not only the corrosion damage progressing into the depth of the material (blue arrow), but also numerous distributed high density intermetallic phases (red arrows) which, when near the surface, are likely to serve as cathodic sites enabling the corrosion reactions.

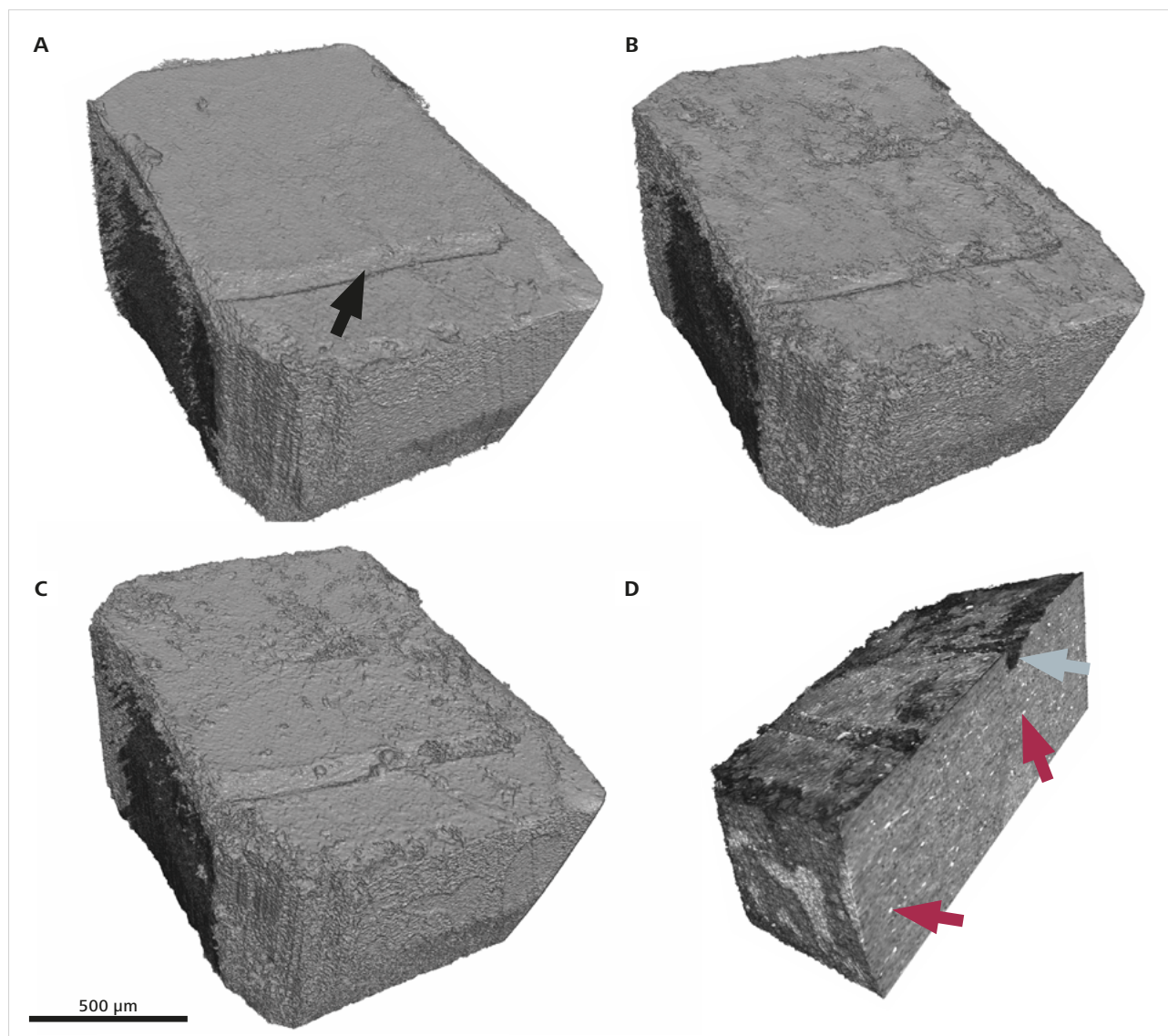


**Figure 3** The sample at various states of corrosion damage as revealed by in situ X-ray microscopy on ZEISS Xradia Versa. a) 2 hours of corrosion, b) 8 hours of corrosion, c) 14 hours of corrosion, d) 14 hours of corrosion, cutaway view of interior structure revealing sub-surface damage (blue arrow) and high density regions (red arrows).

While the information from the *in situ* study at a resolution of  $1\ \mu\text{m}/\text{voxel}$  helps explain the regimes and the overall extent of damage, there is insufficient resolution to reveal information on the detailed corrosion mechanisms, and specifically their connection with the fine length scales of the alloy microstructure. To this end, the Xradia 810 Ultra XRM was used on the extracted region of interest to provide additional information. As this data was collected at the point in time of the approximate transition from Stage 1 to Stage 2 type corrosion behavior, the corrosion front was observed as it first began to consume the internal bulk material. Two orthogonal virtual cross sections are shown in Fig. 4, the locations of which are identified by the lines in the opposing view. The various material phases present in the

sample are identifiable based on their grayscale density. The pores and epoxy appear black. Subsequently, the magnesium hydroxide corrosion product appears as the least dense phase, thereby forming the darkest shade of gray. The magnesium alloy itself appears as a lighter gray, while the brightest regions were a combination of small intermetallic particles, likely containing Al and Mn, and deposited chloride salt (likely mostly NaCl, as confirmed separately by EDS elemental mapping on a different region of the sample) remaining after washing and drying of the sample following the *in situ* experiment. The corrosion was observed to be non-uniform, suggesting the preferential attack of grain boundaries and the associated formation of corrosion product, with likely composition  $\text{Mg}(\text{OH})_2$ . The corrosion

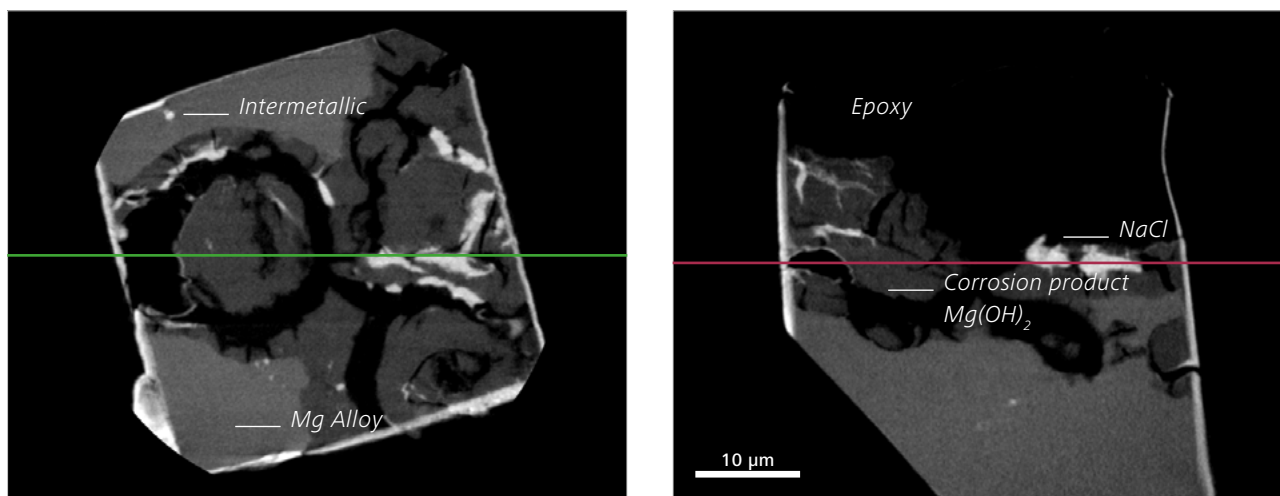


**Figure 4** Nanoscale X-ray microscopy results obtained from ZEISS Xradia 810 Ultra. Two orthogonal virtual cross sections reveal the different solid phases based on density differences, as well as provide insight into the preferential corrosion routes.

product is highly porous and fractured, with very evident cracks and channels spanning from the exposed surface to the underlying pristine Mg alloy, permitting a transport pathway for continued corrosion of the underlying material.

The nondestructive nature of the X-ray techniques could provide the opportunity for continued 4D evolution of the corrosion process at the nanoscale, with repeated scanning using the ZEISS Xradia Ultra microscope. However, this was not performed in this study and is left as a potential topic for future work since the goal of this particular study was to observe the transition from Stage 1 to Stage 2 corrosion in the AZ31 alloy. Rather, the severely corroded grain and grain boundary on the left of Fig. 4 was selected at this point for high resolution FIB-SEM tomography. The FIB-SEM tomography offers resolution an order of magnitude smaller than ZEISS Xradia Ultra XRM, but at the expense of consuming the sample. The data, part of which is shown in Fig. 5, reveals many of the same features as the data from ZEISS Xradia Ultra, as well as a number of finer structures that were not apparent at the coarser resolution. The volume contains intricate crack geometries, some of which have been infiltrated by NaCl, as labeled by the blue arrow. The cracks clearly extend from the surface to the large void towards the bottom of the volume. In addition, the large region of corrosion damage, labeled by the red arrow, shows what appears to be possible varying composition as well as whisker-like features on the exposed surface. These micro-

structural features help provide clues about reaction routes and mechanisms responsible for the corrosion studied here, and could provide valuable insight into the transition between the Stage 1 and Stage 2 corrosion behavior in this alloy.

### Conclusions

This study utilized 3D imaging techniques in a coordinated correlative workflow (via Atlas 5) at the micro and nanoscale to investigate corrosion damage in a magnesium alloy sample. Significant results were as follows:

- Nondestructive X-ray microscopy was used to monitor the corrosion process *in situ* at the microscale.
- Upon observing the transition from 'Stage 1' to 'Stage 2' corrosion, the *in situ* experiment was halted, and the Atlas 5 correlative software environment was used to navigate the ZEISS FIB-SEM to extract a smaller sample from a targeted, highly corroded region of interest.
- Nanoscale X-ray microscopy was performed on the sub-sample, revealing a structure suggesting aggressive grain boundary corrosion and the deposition of fractured, porous corrosion products.
- A smaller sub-region of the Ultra sample was identified and imaged in 3D by FIB-SEM serial section tomography, also performed directly by Atlas 5. Additional fine structures and complex crack geometries were observed, along with a highly irregular distribution of Mg and corrosion products.

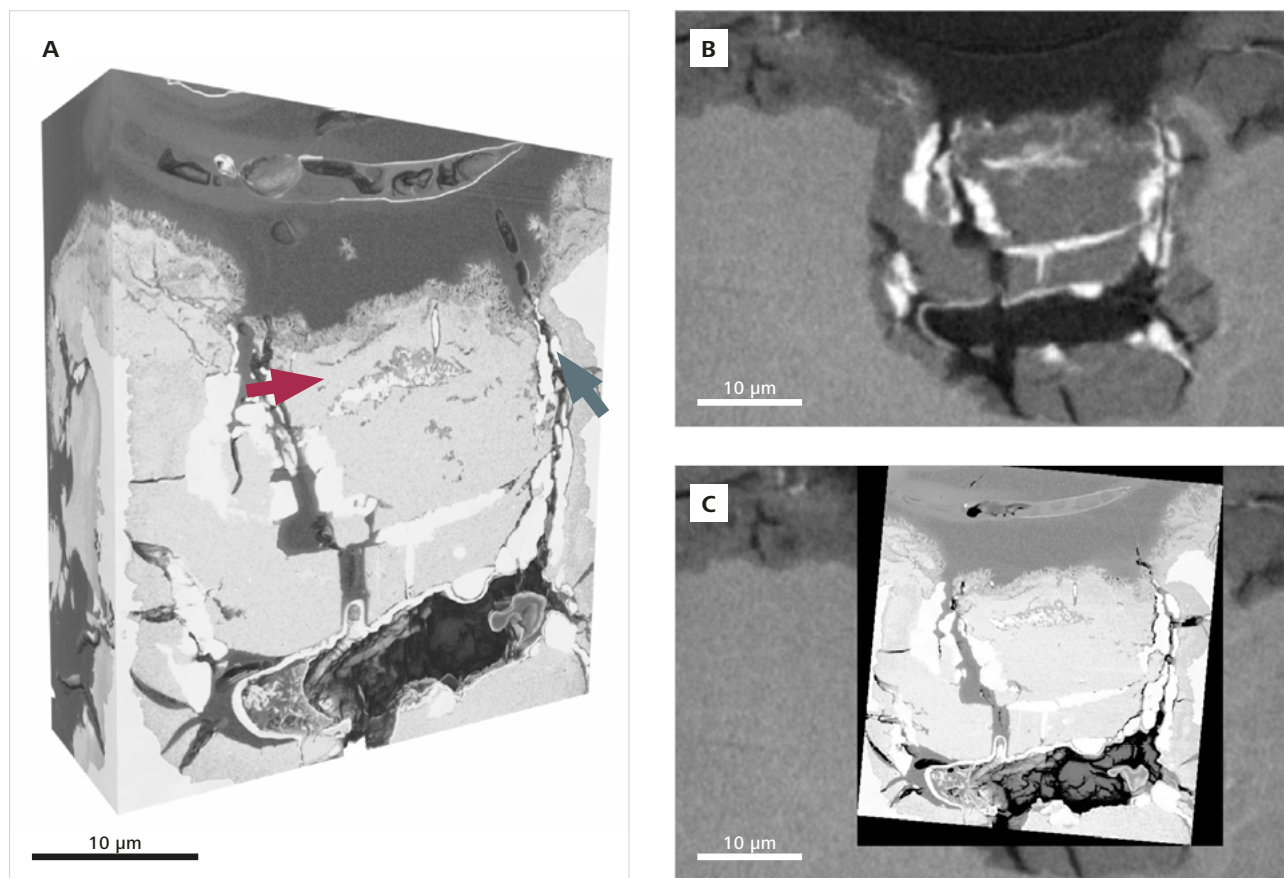


**Figure 5** FIB-SEM tomography. a) A 3D rendering of the volume acquired with FIB-SEM tomography. The data reveals crack geometries and salt deposits (blue arrow) as well as complex corrosion product microstructures (red arrow). b) and c) Comparison of an equivalent 2D plane of data acquired by X-ray microscopy and FIB-SEM tomography.

#### References:

- [1] J. E. Gray, B. Luan, Protective coatings on magnesium and its alloys – A critical review, *J Alloy Compd*, 336 (2002) 88–113.
- [2] M. Curioni, The behaviour of magnesium during free corrosion and potentiodynamic polarization investigated by real-time hydrogen measurement and optical imaging, *Electrochim Acta*, 120 (2014) 284–292.
- [3] S. Pawar et al., The Role of Intermetallics on the Corrosion Initiation of Twin Roll Cast AZ31 Mg Alloy, *J. Electrochem. Soc.*, 162 (2015) C442–C448.
- [4] A. Merkle et al., Automated correlative tomography using XRM and FIB-SEM to span length scales and modalities in 3D materials, *Microscopy and Analysis* (2014) S10–S13.



**Carl Zeiss Microscopy GmbH**  
07745 Jena, Germany  
microscopy@zeiss.com  
www.zeiss.com/microscopy



Not for therapeutic, treatment or medical diagnostic evidence. Not all products are available in every country.  
Contact your local ZEISS representative for more information.

EN\_44\_013\_031 | CZ 01-2019 | Design, scope of delivery and technical progress subject to change without notice. | © Carl Zeiss Microscopy GmbH